High-frequency imaging of a moving object

Clifford Nolan
University of Limerick

Conference in honour of Gunther Uhlmann's 60th Birthday
Irvine, California

21 June, 2012

Outline

- Joint work with Felea and Gaburro.
- Motivated by papers of Cheney and Borden.
- Seek to invert RADAR data for a time-dependent reflectivity function.
- We will see that backprojected RADAR images have artifacts that can be reduced by pre-processing the data.

Static Synthetic Aperture RADAR (SAR)

- In static RADAR we have the following set up:

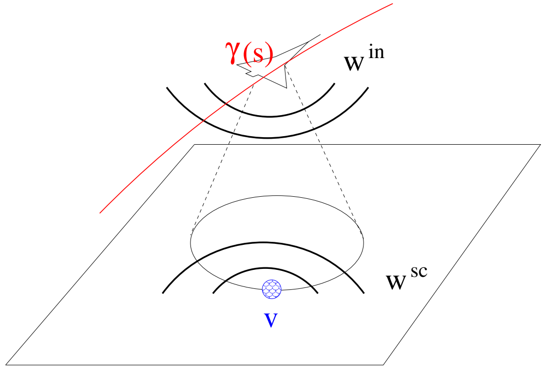

- The object to be imaged ($v(x) := c^{-2}(x) - c_0^{-2}$) is assumed static and the RADAR flies, makes measurements, creating a synthetic aperture
- Backprojection produces an image with standard mirror-artifacts.

Model for moving objects

- Now consider an object which moves as time elapses ...
- Scalar wave equation model for radio waves emitted from location y at time T_y and measured at (x,t):

$$(\Delta - \frac{1}{c^2(x,t)}\partial_t^2)u(y;x,t) = \delta(t+T_y)\delta(x-y)$$

- Notice the time-dependent speed $c(x,t)$.
- Corresponding to this, we build in the flexibility of the initiation time T_y of our RADAR at location y - makes it possible to see multiple facets of object, as it moves.

Linearization

- x is to be thought of as a location of a scatterer in the vicinity of the ground - we consider $x \in \mathbb{R}^2$ or $x \in \mathbb{R}^3$.
- y is to be thought of as the location of the source - we consider $y \in \mathbb{R}^2$ or $y \in \mathbb{R}^3$.
- Linearization: $u(y;x,t) = u^{in}(y;x,t) + u^{sc}(y;x,t)$ where

$$(\Delta - \frac{1}{c_0^2}\partial_t^2)u^{in}(y;x,t) = \delta(t+T_y)\delta(x-y),$$

$$(\Delta - \frac{1}{c_0^2}\partial_t^2)u^{sc}(y;x,t) = v(x,t)\frac{\partial^2 u^{in}}{\partial^2 t}(y;x,t)$$

and

$$v(x,t) := \frac{1}{c^2(x,t)} - \frac{1}{c_0^2}$$

Linearization

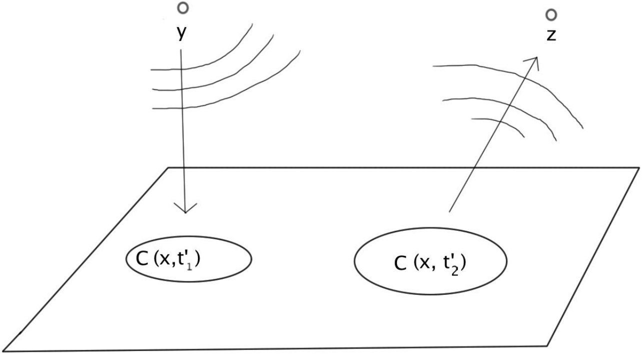

Linearization

- Convolving the source for u^{sc} with the Green's function gives

$$u^{sc}(y;z,t) = \int \frac{\delta(t-t'-\frac{|x-z|}{c_0})}{4\pi|x-z|} \frac{\partial_{t'}^2\delta(t+T_y-\frac{|x-y|}{c_0})}{4\pi|x-y|} v(x,t')dxdt'$$

- We make a simple and concrete choice $T_y = \alpha y_1$, so that sources are fired at different times for different locations along the Y_1 axis.
- We also make a technical but reasonable assumption that $c_0\alpha \neq 1$.

FIO Representation of Scattering Operator F

- Writing δ as an oscillatory integral we arrive at the forward modeling scattering operator F which maps v to u^{sc} as follows

$$Fv(y,z,t) = u^{sc}(y;z,t) = \int e^{i[(t-t'-|x-z|)\omega + (t'+c_0\alpha y_1 - |x-y|)\omega']} \frac{c_0^2\omega^2}{|x-y||x-z|} v(x,t')d\omega d\omega' dx dt'$$

- The operator F can easily be verified to be a Fourier Integral Operator (FIO) of order q, say.

Summary of Results

- We consider the model $v(x,t') \in \mathcal{E}'(X)$ where $X := \mathbb{R}^m$ and the data $Fv(y,z,t) \in \mathcal{E}'(Y)$ where $Y := \mathbb{R}^d$.
- Since F is a FIO, it has a canonical relation $C \subset T^*Y \times T^*X$, which describes how F maps singularities in v to singularities in u^{sc}.
- The acquisition geometry determined in part by m, d strongly influences the structure of the relation C and we now consider some explicit geometries ...
- In all cases we consider the natural projections $\pi_L : C \longrightarrow T^*Y, \; \pi_R : C \longrightarrow T^*X$

Summary of Results

- Case 1: The "deluxe" data case: y, z, x belong to bounded subsets of $\mathbb{R}^3$
- In this case, $d = 7, m = 4$.
- $\Rightarrow \pi_L$ an embedding (and π_R a submersion).
- $\Rightarrow F^*F$ is a microlocally elliptic ΨDO (by Guillemin's result)
- Therefore, F has a left-parametrix and this is the nicest possible case - but expensive to collect and invert data.

Summary of Results

- Case 2: Same as case 1 but the source and receiver are coincident $y = z$.
- This is a formally determined case ($d = m = 4$).
- π_L and π_R both have blowdown singularities (more on this later).
- If we apply F^* to the data, we show that artifacts appear which **can be more singular** than the true singularities.
- This follows from K_{F^*F} belonging to the class $I^{\frac{5}{2},-\frac{1}{2}}(\triangle, \Lambda)$ (more on this later).

Summary of Results

- Case 3: Same as case 2 but $y_3 = z_3$ are constant and the scatterer is assumed to be on the ground $x_3 = 0$.
- This is a formally determined case $(d = m = 3)$.
- π_L and π_R both have blowdown singularities.
- If we apply F^* to the data, we show that artifacts appear which **can be just as singular** as the true singularities.
- This follows from K_{F^*F} belonging to the class $I^{3,0}(\triangle, \Lambda)$.

Summary of Results

- Case 4: $y_3 = z_3$ are constant. $y_2 = z_2$, $y_1 \neq z_1$, no restriction on scatterer location.
- This is a formally determined case ($d = m = 4$).
- π_L and π_R both have blowdown singularities.
- If we apply F^* to the data, we show that artifacts appear which **can be just as singular** as the true singularities.
- This follows from K_{F^*F} belonging to the class $I^{2,0}(\triangle, \Lambda)$.

Ingredients of Analysis

- The results for case 1 are easily understood.
- For cases 2-4 we find that π_L, π_R have a blowdown singularity along a submanifold $\Sigma \subset C$.
- For π_L for example, this means that (i) π_L drops rank by $k > 0$ at Σ, (ii) $Ker(D\pi_L|_\Sigma) \subset T\Sigma$ and (iii) $det(D\pi_L)$ vanishes to order k at Σ.
- Canonical form of a blowdown:
  $f(x_1, \ldots, x_{n-k}, x_{n-k+1}, \ldots, x_n) =$
  $(x_1, x_2, \ldots x_{n-k}, x_{n-k+1}x_1, \ldots, x_n x_1)$
- We are able to apply a theorem of Marhuenda which states that if π_L, π_R only have blowdown singularities at Σ and $\pi_L(\Sigma), \pi_R(\Sigma)$ are involutive and non-radial, then the distribution kernel $K_{F^*F} \in I^{2q+(k-1)/2,-(k-1)/2}(\triangle, \Lambda_{\pi_R(\Sigma)})$.
- The 'artifact' manifold $\Lambda_{\pi_R(\Sigma)}$ is as follows ...

Ingredients of Analysis

- As stated $\pi_R(\Sigma)$ is involutive, which roughly means its homogeneous defining functions are given by equations of the form $\xi_i = 0, \ i = 1, \ldots r$ for some $r > 0$ with $\{\xi_i, \xi_j\} = 0, i, j = 1, \ldots, r$.
- The artifact submanifold $\Lambda_{\pi_R(\Sigma)}$ is the joint flow-out from Σ by the Hamiltonian vector fields $\{H_{\xi_i}\}_{i=1}^r$.
- Note that $u \in I^{p,l}(\Delta, \Lambda) \Rightarrow u \in I^{p+l}(\Delta \setminus \Lambda)$ and $u \in I^p(\Lambda \setminus \Delta)$ which leads to the results about the strength of the artifact singularities that we quoted.

- For example, in case 4, Σ is defined by the single equation:

$$\frac{\omega'}{|x-y|} + \frac{\omega}{|x-z|} = 0$$

$$C = \Big\{ y_1, y_2, z_1, t, c_0\alpha\omega' + \omega'\frac{x_1-y_1}{|x-y|}, \omega'\frac{x_2-y_2}{|x-y|} + \omega\frac{x_2-y_2}{|x-z|}, \\ \omega\frac{x_1-z_1}{|x-z|}, \omega; x_1, x_2, x_3, t', \omega'\frac{x_1-y_1}{|x-y|} + \omega\frac{x_1-z_1}{|x-z|}, \\ \omega'\frac{x_2-y_2}{|x-y|} + \omega\frac{x_2-y_2}{|x-z|}, \omega'\frac{x_3-h}{|x-y|} + \omega\frac{x_3-h}{|x-z|}, \omega-\omega', \Big\}$$

with the travel time conditions

$$t' = -c_0\alpha y_1 + |x-y| \qquad ; \qquad t = -c_0\alpha y_1 + |x-y| + |x-z|.$$

- In this case, $K_{F^*F} \in I^{2,0}(\Delta, \Lambda_{\pi_R(\Sigma)}) \Rightarrow K_{F^*F} \in I^2(\Delta \setminus \Lambda_{\pi_R(\Sigma)})$, $K_{F^*F} \in I^2(\Lambda_{\pi_R(\Sigma)} \setminus \Delta)$

Reduction of Artifacts

- The previous slide indicates that artifacts will flow out from Σ.
- However, we can preprocess the data and reduce the strength of the artifacts as follows.
- We construct a zero order ΨDO, namely Q such that it's principal symbol σ_Q vanishes to order $s \geq 1$ on $\pi_L(\Sigma)$.
- It then follows from the $I^{p,l}$ calculus (Greenleaf, Uhlmann, Marhuenda) that $F^*Qd = F^*QFv \in I^{2q-s+(k-1)/2, s-(k-1)/2}(\cdot,\cdot)$.
- In case 4, $K_{F^*QF} \in I^{2-s,2}(\Delta, \Lambda_{\pi_R(\Sigma)}) \Rightarrow K_{F^*QF} \in I^2(\Delta \setminus \Lambda_{\pi_R(\Sigma)}),\ K_{F^*QF} \in I^{2-s}(\Lambda_{\pi_R(\Sigma)} \setminus \Delta)$
- For example in case 3, $Q = (\partial_{y_2}^2 + (\partial_{y_1} + \partial_{y_3})^2)(-\Delta)^{-1}$.

Concluding Remarks

- We have shown that it is possible to image moving objects and that unless a high-demensional data set is used (case 1), or else a filtered backprojection is employed, strong artifacts can occur in the back projected image.
- A more practical consideration / implementation of this method would be useful.